Available on CMS information server **CMS NOTE 1997/013**

The Compact Muon Solenoid Experiment

CMS Note

Mailing address: CMS CERN, CH-1211 GENEVA 23, Switzerland

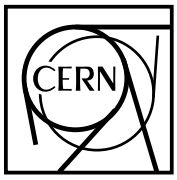

March 18, 1997

Proposal for the read-out electronics of gas micro-strip detectors in the CMS tracker

J.-F. Clergeau, V. Chorowicz, D. Contardo, R. Haroutunian, L. Mirabito, S. Muanza, G. Smadja

IPN Lyon, France

Abstract

The signal of minimum ionizing particles, crossing perpendicular MSGC's at LHC frequency, was simulated to propose a suitable read-out scheme for the gas micro-strip detectors of the CMS tracker.

1 Motivation and status of the study

The RD20 scheme [1] is the baseline design for the read out of the silicon and gas micro-strip detectors in the CMS tracker. It includes a fast amplifier and shaper, an analogue delay buffer, a pulse shape processor and a multiplexer. While these functions have been implemented in the APV [2] and FILTRE [3] chips with characteristics adapted to the signal of silicon detectors, the analysis of experimental data has shown that the fluctuations in the charge collection with MSGC's or MGC's will reduce the performance of these chips [4],[5].

A signal simulation [6] was used to study the effect of the front-end shaping, of the analogue delay buffer dynamic range and of various processing algorithms. The assumptions, the results and the propositions for a micro-strip gas detector read-out are presented.

2 Simulation tools and assumptions

The simulation, as compared to the study of actual data [4],[5], allows to test the effect of different shapings on the pulse processing, taking into account the pile-up on individual strips. These three steps, pulse shape generation, pile-up simulation and processing are described in this section.

2.1 Track pulse generation

The detailed description of the pulse simulation can be found in reference [6]. It consists in the generation of the input current of the preamplifier and its convolution with a given shaping. The current is simulated for perpendicular MIP's, including primary ionization, migration, diffusion and avalanche gain. In this simulation, the parameters involved were adjusted so as to reproduce the mean characteristics of real pulse shapes, registered with a MSGC equipped with the PRESHAPE32 front-end [5]. For the 10000 tracks generated, the currents shared on different strips (cluster) are representative of the signal developing in a gas mixture of DME(80%) and CF_4(20%) with gaps of either 2 mm or 3 mm and at a drift field of 8.6 kV/cm. With other gas mixtures, differences can arise from changes in the primary ionization, in the drift velocity and in the diffusion. The latter aspect is not of primary importance since the cluster size with the thresholds currently applied are similar for the usual gas mixtures. The fluctuations in the primary ionization will be relatively small if a large amount of DME is used. As shown in reference 5, the variations in the electron drift velocity can modify the shape of pulses, leading to a mean peaking time variation of about 10 ns. In this respect, the fast gas mixtures should be preferred. A recent measurement of pulses with DME(70%) and Ne(30%) shows that the mean shape of the pulses is similar to the one used to adjust the parameters of the simulation. It is thus expected that in this case the results of the processing will not be modified.

The convolution of the simulated currents with the shaper amplifier response provides the final pulses. The impulse response of the PRESHAPE32 chip was adjusted, with the bias voltages, so as to exhibit a 40 ns peaking time with the 12 pF load capacitance of the detector strips. It was used as a reference for comparison with CR-RC shapings of 20 ns, 30 ns, 40 ns, 50 ns and 75 ns time constants. It can be seen on figure 1a that the CR-RC response with a 30 ns time constant is the closest to the PRESHAPE32 case.

2.2 Pile-up simulation

Three track multiplicities per bunch crossing were simulated : 0.5%, 1%, and 5% of the number of channels in the tracker, assumed to be 4 x 10^5.

The pulses from a bunch crossing considered in the processing (referenced as the trigger bunch crossing in the following), were added to the tails of pulses generated in 35 bunch crossings occuring before and after, at the 40 MHz frequency of the LHC.

The noise, as observed in the data measured with the PRESHAPE32, was then added to all the tracker channels. Before the addition, the signals of MIPs were normalized arbitrarily to study the effect of different signal to noise ratio. This latter variable is defined as the maximum probability amplitude on the highest strip of a cluster divided by the noise rms. The tested values were 10, 25 and 50.

Using an amplitude calibration of the PRESHAPE32 measured with a buffer of gain 10 and the load capacitance of the detectors, the 4.5 mV rms value of the noise is equivalent to 1400 e^-. Therefore, for a signal to noise ratio of 25 the equivalent signal seen by the amplifier is 35000 e^- (-112 mV). This measured value [5], although not final, can be considered as a good specification for the signal of the MSGC detectors in the CMS tracker.

2.3 Pulse processing

To take into account both the effect of the pile-up and of the electronics noise in the final occupancies, the signals on all the tracker channels were processed. Results are reported for processings using three samples of the pulses with time intervals of either 25 ns or 50 ns.

The tested algorithms are a weighted sum, a rise selection, a shape selection and a peak identification. Each of them can be tuned with two parameters, weights for the weighted sum and thresholds for the other algorithms (see appendix).

A finite dynamic range was simulated by saturating the pulses before the processing. Four cases were tested, no saturation and saturations at 140000 e^- (-450 mV), 210000 e^- (-675 mV) and 280000 e^- (-900 mV).

3 Performance of the different read-out schemes

3.1 Definition of the performance variables

The result of the processing is a number of identified clusters including true tracks, either generated in the trigger or surrounding bunch crossings, and false tracks due to the electronics noise. In the following, the performance of the read-out is represented by the efficiency to preserve the clusters associated to the trigger bunch crossing tracks, plotted against the total number of clusters divided by the number of tracker channels (referenced as the final occupancy in the following).

A cluster is defined as a group of adjacent strips, presenting individually a processed amplitude above a first level threshold, and a sum 1.5 times higher than this threshold. This selection is in current use in off-line analysis of MSGC data.

For each pair of algorithm parameters, a curve of efficiency versus occupancy is obtained according to the cluster selection threshold. In the following, we plot the envelope of these curves, which corresponds to the best values of efficiency and occupancy found, whatever the values of the algorithm parameters and of the cluster selection threshold.

Since only perpendicular MIP's and noise are included in this simulation, the scales of efficiency and occupancy are not quite representative of the LHC conditions but are expected to be relevant for the comparison of the relative performance of the proposed read-out schemes. To complete the study, we present the spatial resolution obtained in few cases.

3.2 Results according to the shaping time constant

The means of the simulated pulses with various shapings are shown in figure 1b for the strip of the cluster with the highest signal. It can be seen that the charge collection in the detector increases the mean peaking time of the shaping by about 40 ns (DME(80%)/CF_4(20%), 3 mm). The processed signals are thus spread over an increasing number of bunches when the shaper time constant increases. As a general consequence, the performance of the processing tends to improve with decreasing time constants.

The results presented in figure 2 show that the peak identification is the method least sensitive to the shaping. In the simulation, the same signal to noise ratio was assumed for the different shapings. Since the electronics noise usually increases with decreasing time constant, the improvement reached with the shortest shaping time can depend on the capability to balance this effect by an equivalent increase of the signal. On the other hand, the reduced performance observed with the largest time constants will probably not be compensated by a decrease of the noise for a signal to noise ratio above 25 (see fig. 2 and 4). Therefore, the shaping realised with the PRESHAPE32 chip is considered as a good compromise. It has to be noted that changes of the shaping time due to the detector itself (strip capacitance and collection time of primary electrons) will result in similar effects as changes in the preamplifier shaping time constant.

3.3 Results according to the time interval between the samples

The pulse sampling has to be done with the 25 ns period of the LHC bunch crossings to ensure a good synchronization with the trigger. The time intervals between the amplitudes used in the processing can thus only be multiple values of 25 ns.

With the weighted sum, the shape selection and the peak identification it was found that the best results are obtained when the second sample is taken close to the pulse maximum amplitude and separated by 50 ns from the two other

samples (fig. 3). This result is independent of the shaping. The algorithm the least sensitive to the time interval is the weighted sum.

With the rise selection the choice of the best time interval is dependent on the shaping. With the PRESHAPE32 chip, the optimization is reached when the second sample is taken at half the pulse maximum amplitude and with a time interval of 25 ns ensuring that the three processed amplitudes are in the rising edge of the pulses. For this same reason, a time interval of 50 ns becomes better if the shaping time constant exceeds 40 ns.

The following comments can be added to the discussion of the time interval between the processed amplitudes :

- Attempts to use a time interval of 75 ns, even if limited to 2 of the 3 samples, have failed to provide good results because the pile-up increases more than the efficiency for the trigger tracks.

- Attempts to increase the number of samples in the processing to 4 were no more successful, although not exhaustive of all the possible variants of algorithms and time samplings. In some cases, for instance with a 50 ns sampling, the fourth amplitude falls close to the noise level. In other cases, a reduction of the sampling time to 25 ns reduces the amplitude differences and thus the track efficiency.

3.4 Effect of the signal to noise ratio and of the dynamic range

In the case of the PRESHAPE32 chip, the effect of the signal to noise ratio and of a finite dynamic range on the processing performance are shown respectively in figure 4 and 5.

It can be seen that when the signal to noise ratio increases from 25 to 50, the processing does not significantly improve in the case without saturation and is even worsened if the available dynamic range is smaller than 280000 e^-. On the other hand, at a signal to noise ratio of 10, the dynamic range is not important in the limit of 140000 e^- but the efficiency is reduced by 2 % to 5 % in this case. The peak identification algorithm is the least sensitive to the signal to noise ratio.

To complete the study, an electronics noise increased by a factor 2 (2800 e^-) was assumed, with a signal of 35000 e^- (S/N = 12.5) and 70000 e^- (S/N = 25). The results are compared to the situation of 35000 e^- and S/N = 25 in figure 6. It can be seen that the efficiency loss if the noise is doubled is compensated by an equivalent increase of the signal only if the dynamic range is 280000 e^-.

An increase of the signal to noise ratio above 25, even if not strictly needed to improve the efficiency, could however improve the cluster size (spatial resolution for perpendicular tracks) and the efficiency for slant tracks. In this latter case, the expected limitation comes from the lower signal to noise ratio on individual strips and from the time jitter between the signals collected on the strips where the particles enter and leave the gas gap.

3.5 Comparison of the performance of the processing algorithms

In the case of the PRESHAPE32 shaping, the performance of the algorithms is compared in figure 7 for the various conditions used in the simulation and a gas gap of 3 mm. In fig 8 the comparison is limited to the peak identification and the rise selection. It is done in the case of a 1 % occupancy for various signal to noise ratios and for two gas gaps of 2 mm and 3 mm in the case of the rise selection. The results can be summarized as follows :

a) Weighted sum

This method is worse than algorithms based on sample comparisons, unless the signal to noise ratio is sufficient (25) and the final occupancies are large, 2.5 % and 10 % for initial occupancies of respectively 1 % and 5 %.

b) Shape selection

As compared to others, this algorithm is better to reject the tracks produced around the trigger bunch crossing but the efficiency for the trigger tracks is limited by the pile-up. It provides the best results only for a final occupancy below 0.8 % and 1.6 %, if the initial occupancy is respectively 0.5 % and 1 %.

c) Peak identification

Less selective than the shape algorithm but more efficient for the trigger tracks, the peak identification provides the best results in the mid-range of efficiency and occupancy. With a 3 mm gap it is worse than a rise selection if the initial occupancy is 5 %.

d) Rise selection

More sensitive to the signal to noise ratio, but less to the initial occupancy, the rise selection becomes less efficient

than the peak identification at a signal to noise ratio below 22, an occupancy of 1 % and a gas gap of 3 mm. The sensitivity of this algorithm to the shaping is, as compared to the others, an advantage with a 2 mm gap where the signal peaking time is well adapted to a time interval of 25 ns between the processed samples. As a consequence, when the initial occupancy is 1 % and the noise 1400 e^-, the results obtained with a 2 mm gap and the rise selection becomes better than any results with 3 mm, at a same gain corresponding to signal to noise ratios of 13 and 20 respectively for the 2 mm and 3 mm gap.

4 Summary and conclusions

The present study has explored different scenarios of the read-out scheme and experimental operation of the micro-strip gas counters in the CMS tracker. It has shown that there is not a clear-cut solution for the best read-out scheme since the performance depends on parameters which are not yet final :

- the time development and amplitude of the detector signal;

- the electronics shaping, noise and dynamic range;

- the initial occupancy, the chosen compromise between efficiency and final occupancy and the expected resolution.

The last point is a matter of simulation where the choices should be determined according to the track reconstruction efficiency and momentum resolution. To estimate these variables, a realistic simulation of proton or heavy ion collisions is needed especially to introduce real track angles and energies. These aspects have not been included in the present study. Assuming that they will not change the relative results that have been presented, the following scheme for the read-out of the gas detectors can be proposed.

4.1 Shaper amplifier

As demonstrated in section 3.2 the shaping implemented in the PRESHAPE32 chip is satisfactory. A larger shaping will penalize the performance, especially if the strip load capacitance is increased or for any other reason of increase in the time development of the signal. With a shorter shaping, although potentially better, it should be proven that the signal to noise ratio is preserved.

4.2 Dynamic range

The study was done assuming the saturation of the pulses as presented in section 3.4. It is shown, when the maximum probability signal on a strip is 35000 e^- and the noise rms is 1400 e^-, that the performance of the read-out will decrease for an effective dynamic range below 140000 e^-. It is also shown, that increasing the detector gain, for instance to compensate an increase by a factor two in the noise rms, will not be efficient unless the dynamic range is also doubled.

An effective range of 140000 e^- (pedestal subtracted) is therefore reasonable if the 1400 e^- rms noise and 35000 e^- signal are guaranteed but it will not allow much improvement in the detector gain (especially if needed to improve the efficiency for inclined tracks). Finally, the read-out of both anodes and cathodes for a measurement of two coordinates requires that the dynamic range should work in two polarities.

4.3 Processing algorithm

The performance of any simulated algorithm is related to the choice of a good set of parameters which are dependent on the exact operating conditions. These parameters should therefore be adaptable together with the timing of the analogue delay buffer clock and the cluster selection threshold. The tuning procedure has to be determined. The simulation of LHC events can be used to provide a first set of values to be checked with data. In this latter step, the identification of trigger tracks should be done with the pixel and silicon detectors to provide the corresponding efficiency in the gas detectors as a function of the final occupancy. The procedure might be iterative to find the best performance. Depending on the particle multiplicity, it is not excluded that the final parameters could vary according to the radial position of the detectors.

The conclusions on the performance of the various processing algorithms are the following :

Apart from the case of high occupancies, the weighted sum performs worse than the comparison of samples. It provides its best results with a time sampling of 50 ns and no obvious correlation was found between the weights themselves and with the final cluster selection threshold. An example of the performance for three specific sets

of weights is shown in figure 9 together with the expected resolution. This processing, foreseen for the silicon detectors, could be a back-up solution if the comparator based algorithms can not be implemented properly in a chip or if the highest initial occupancy is expected.

The implementations in the chip of the three proposed methods of comparison are not very different. However, the adapted time sampling should be 50 ns for a shape or a peak identifications and 25 ns for a rise selection (PRESHAPE32 shaping).

The peak and rise algorithms provide better results than the shape identification on a wider range of occupancies and efficiencies. They are therefore preferable in general.

A definite choice between the peak identification and the rise selection is more specific to the expected experimental conditions. The 2 mm gap with the rise selection is the most promising contrivance. It should however be checked experimentally if a signal to noise ratio above 13 and the simulated shaping can be ensured and are sufficient with such a gap. The situation with a cathode read-out for a measurement of the two coordinates may require another algorithm given these restrictions. If a 3 mm gap is preferred, the peak identification is less sensitive to the shaping and provides better results if the signal to noise ratio is below 22. It could thus be well suited unless high occupancies are considered.

The present simulations do not include common mode noise in the read-out electronics. The results presented thus assume that if present, it can be subtracted before applying a final threshold on the transferred amplitudes. A weighted sum of pulse samples will preserve the common mode noise for all the tracker channels. It can therefore be subtracted, but with a possible limitation due to the pile-up and to the cross-talk between the strips that can result in base line fluctuations. These physical effects can be enhanced with the weighted sum which introduces an overshoot (reverse polarity) of the pulses for tracks produced in the bunch crossings surrounding the trigger bunch crossing.

In the case of the sample comparisons, only the accepted amplitudes are preserved and the part of the common mode noise generated before the processing, if any, is lost. One possible solution to preserve its value is to transfer both the peak amplitude and the validation by the processing, before the final cluster selection. It should be checked if the read-out frequency allows such a transfer. Another possibility is to replace the amplitude validation by a baseline shift according to the output of the comparison. In this case, it should be checked if the dynamics can be doubled or if the signal can be compressed by a factor 2 without too much loss on the signal to noise ratio. A comparison of the performance with an without common mode noise subtraction has been simulated. The situation where the common mode noise can be subtracted assumes as mentionned before that it appears on all the channels after the processing, it is represented by the open circles in figure 10. The situation without common mode noise subtraction is equivalent in the case of the peak selection to set the final threshold on the transferred amplitudes to 0, it is represented by the full circles in figure 10. With the rise selection, one possibility is to validate the amplitude difference between the third sample used in the processing (close to the pulse maximum) and a sample taken before the rising edge (25 ns before the first one used in the processing). In this case the common mode noise is subtracted in the difference of the two samples and the final threshold can be applied, the performance loss is only due to an increase of the noise by a factor $\sqrt{2}$. With these two exemples, it can be seen in figure 10 that the performance without common mode noise subtraction is degraded at maximum by about 0.5 %, at a bunch crossing pile-up of 2.1. Furthermore, The spatial resolution is almost unaffected.

The reported spatial resolutions are obtained assuming an analogue treatment of the data (center of gravity of cluster strip signals). They are quite similar for the various processing algorithms and close to the value expected with a digital read-out. This is due to the low efficiency for the second or third strip of a cluster, which often present a small signal, and to the limited amplitude resolution, which is affected by the effect of the processing and by the pile-up of signals. In the present study, the cluster size is defined with a same threshold for all the strips, another possible method is to make a first similar selection of strips and then define the final clusters with neighbouring strips presenting a signal above a lower threshold. This might improve the spatial resolution but is not expected to modify the efficiencies or the occupancies which are basically determined by the first selection of strips with a higher threshold.

4.4 Proposal for the read-out electronics

This proposal concerns only the case of the comparator solutions which have not yet been implemented in a chip. As discussed above, the choice between the peak or the rise algorithm is not obvious. It is suggested to benefit from their similarities to implement both of them in the same read-out electronics. This is possible with the schematics chip shown on figure 11 if a peak or rise mode can be selected to choose one of the two samples at the input of each comparator. With five samples numbered one to five issued of the analogue delay buffer and separated by 25 ns,

the chip will act as a peak finder, if its entries 1 to 5 are respectively the samples 3, 3, 1, 3 and 5 and as a rise finder if they are respectively the samples 3, 2, 1, 3, 2.

Finally, the test of a read-out chip, whatever the processing algorithm, will be difficult to achieve without a test beam synchronized to the 25 ns clock and an intensity able to reproduce the pile-up at LHC. A practical solution for tests in the laboratory could be to have a test output at the level of the shaper amplifier and a test input at the level of the analogue delay buffer. This will allow to check the signal shape and simulate, with a 40 MHz generator, realistic samples including the pile-up effect, that can be stored in the analogue delay buffer and processed.

Acknowledgment

We thank G. Hall for corrections and helpful criticism.

References

[1] RD20 Status Report CERN/DRDC 94.39 (1994).

[2] CMS TN/94-320, G. Hall.

[3] CMS IN/1996-004, U. Goerlach et al..

[4] J.F. Clergeau et al., Nucl. Inst. and Meth. A355 (1995) 359.

[5] F. Angelini et al., Nucl. Inst. and Meth. A368 (1996) 345.

[6] J.F. Clergeau et al., Lycen/9630 (1996).

Appendix

The description of the processing algorithms is done assuming that the pulses are of negative polarity.

1) **Peak identification**

The output amplitude is given by :

$$S = S(t_0) \quad \text{if} \quad \begin{cases} S(t_0) < S(t_0 - \Delta t) - th_1 \\ S(t_0) < S(t_0 + \Delta t) - th_2 \\ S(t_0) < -th_3 \end{cases}$$

and $S = 0$ otherwise,
t_0 is the trigger time, Δt is the sampling time and th_1, th_2, th_3 are thresholds.

2) **Shape identification**

The output amplitude is given by :

$$S = S(t_0) \quad \text{if} \quad \begin{cases} S(t_0) < S(t_0 - \Delta t) - th_1 \\ S(t_0 + \Delta t) < S(t_0 - \Delta t) - th_2 \\ S(t_0) < -th_3 \end{cases}$$

and $S = 0$ otherwise,
t_0 is the trigger time, Δt is the sampling time and th_1, th_2, th_3 are thresholds.

3) **Rise selection**

The output amplitude is given by :

$$S = S(t_0) \quad \text{if} \quad \begin{cases} S(t_0 - \Delta t) < S(t_0 - 2\Delta t) - th_1 \\ S(t_0) < S(t_0 - \Delta t) - th_2 \\ S(t_0) < -th_3 \end{cases}$$

and $S = 0$ otherwise,
t_0 is the trigger time, Δt is the sampling time and th_1, th_2, th_3 are thresholds.

4) **Weighted sum**

The output amplitude is :
$S = W_1 \cdot S(t_0 - \Delta t) + W_2 \cdot S(t_0) + W_3 \cdot S(t_0 + \Delta t)$ if $S < -th$,
and S= 0 otherwise,
t_0 is the trigger time, Δt is the sampling time and W_1, W_2, W_3, th are the weights and the threshold.

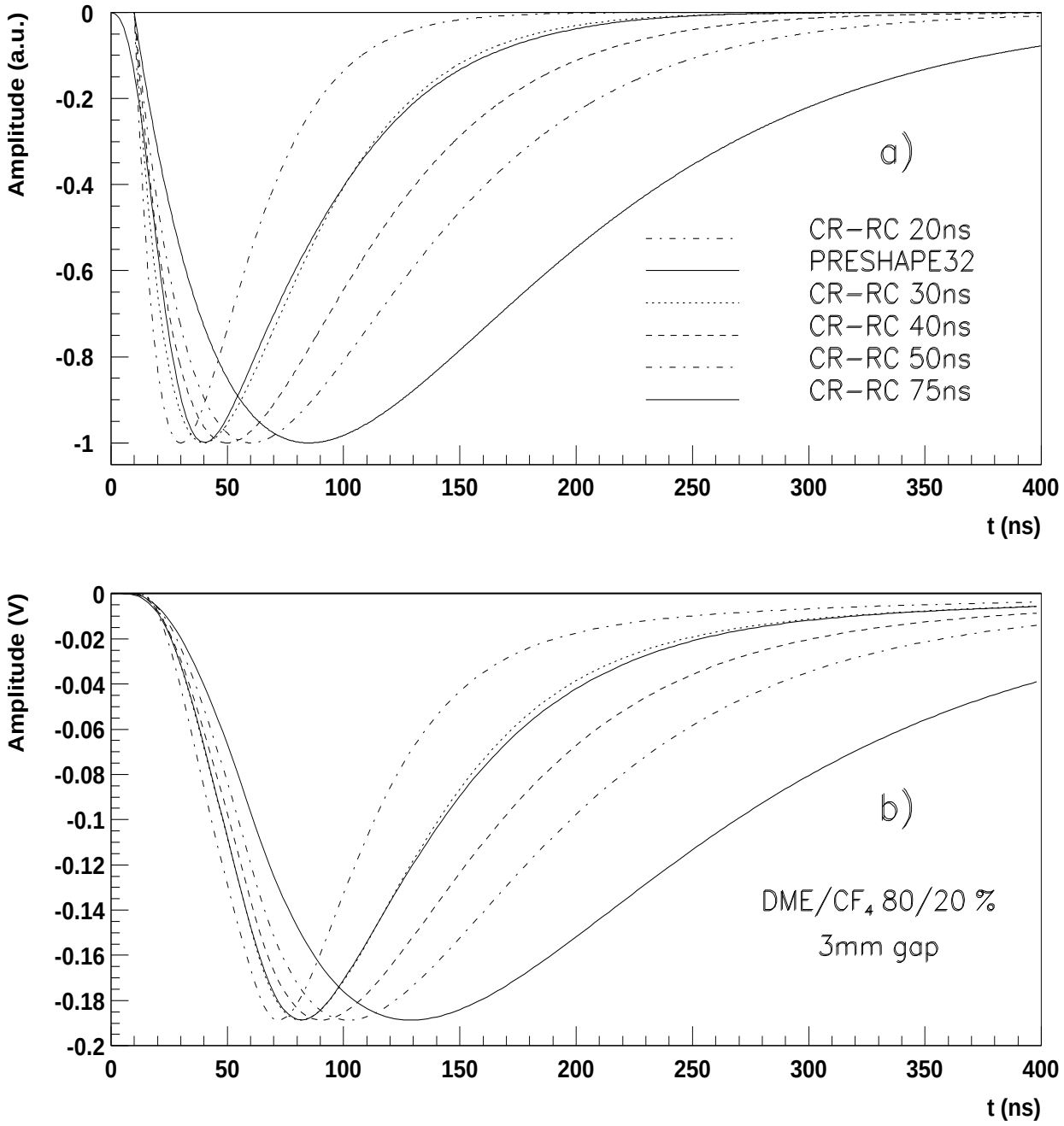

Figure 1

(a) PRESHAPE32 response to a fast generator with the detector load capacitance and theoretical CR-RC shapings.
(b) Means of the pulses simulated with the various shapings for the cluster strip with the highest signal.

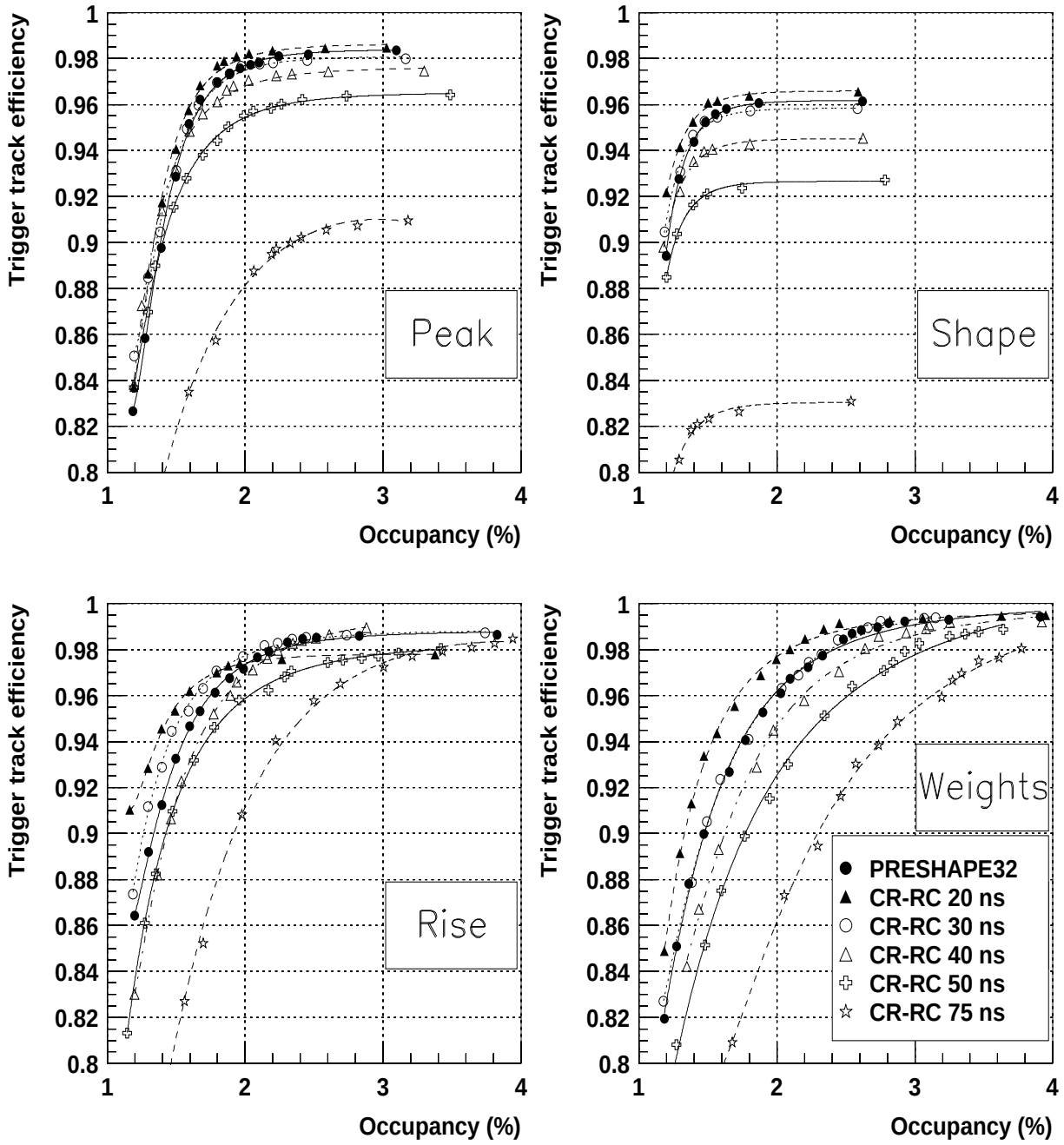

Figure 2

Comparison of the algorithms performance with various shapings. The signal is 35000 e^-, the noise rms is 1400 e^- and the detector initial occupancy is 1% (see definitions in text).

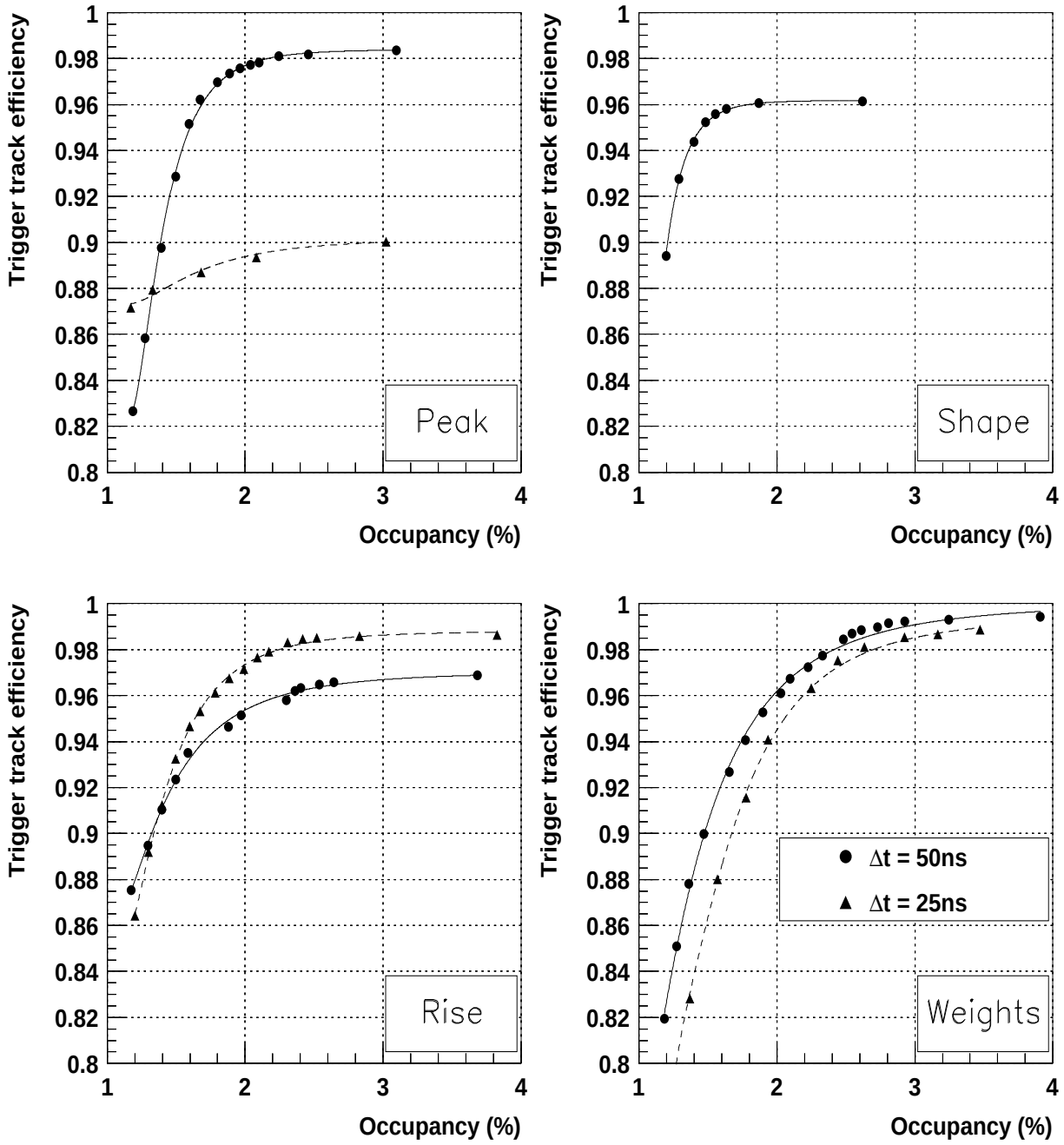

Figure 3

Performance of the various algorithms with 25 ns and 50 ns time intervals between the processed samples in the case of the PRESHAPE32 shaping. The signal is 35000 e^-, the noise rms is 1400 e^-, the detector initial occupancy is 1% (see definitions in text).

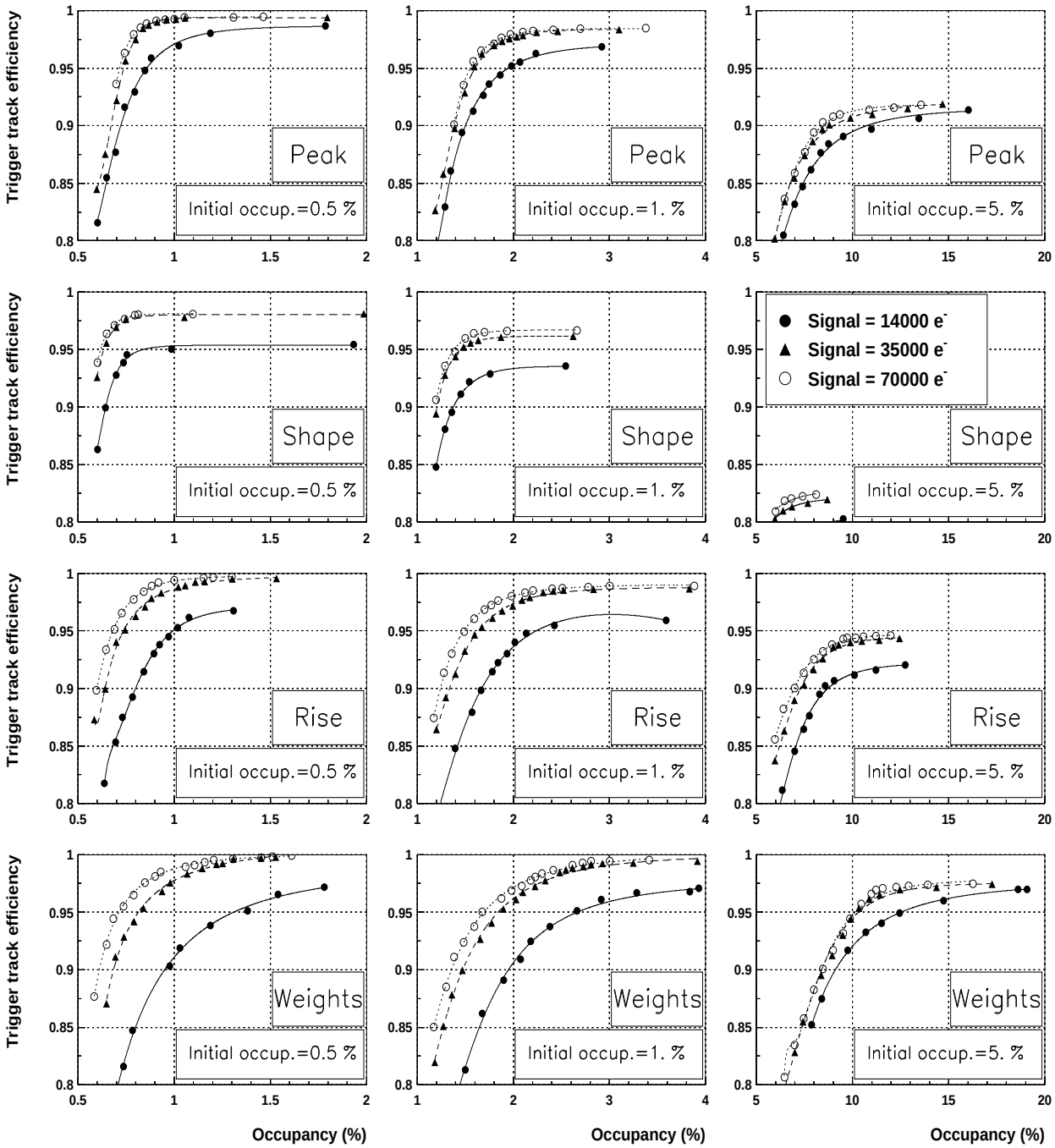

Figure 4

Performance of the various algorithms as a function of the signal to noise ratio and the initial occupancy in the case of the PRESHAPE32 shaping. The noise rms is 1400 e^-.

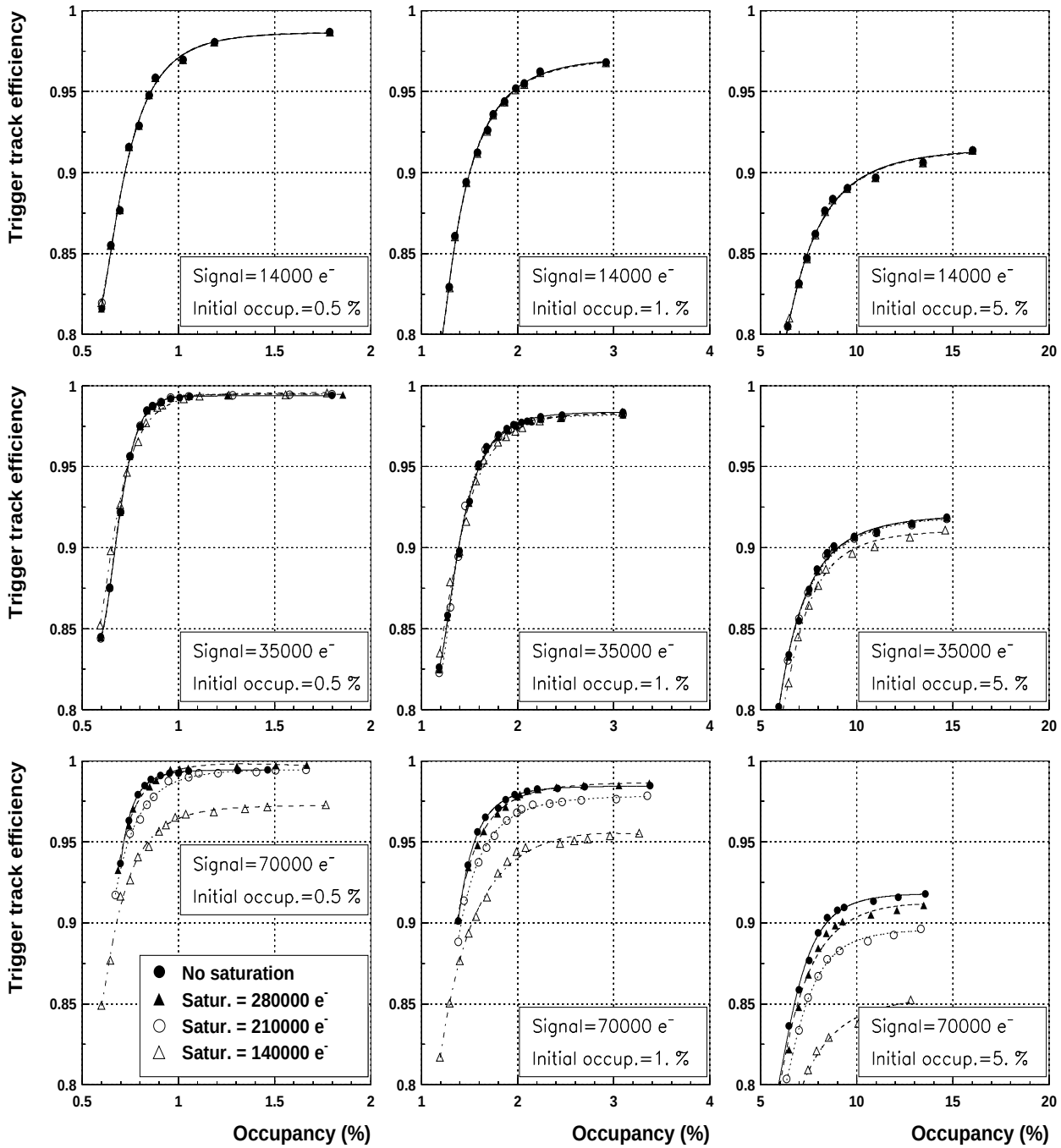

Figure 5a

Effect of the dynamical range on the performance of the peak identification algorithm in the case of the PRE-SHAPE32 shaping. The noise rms is 1400 e^-.

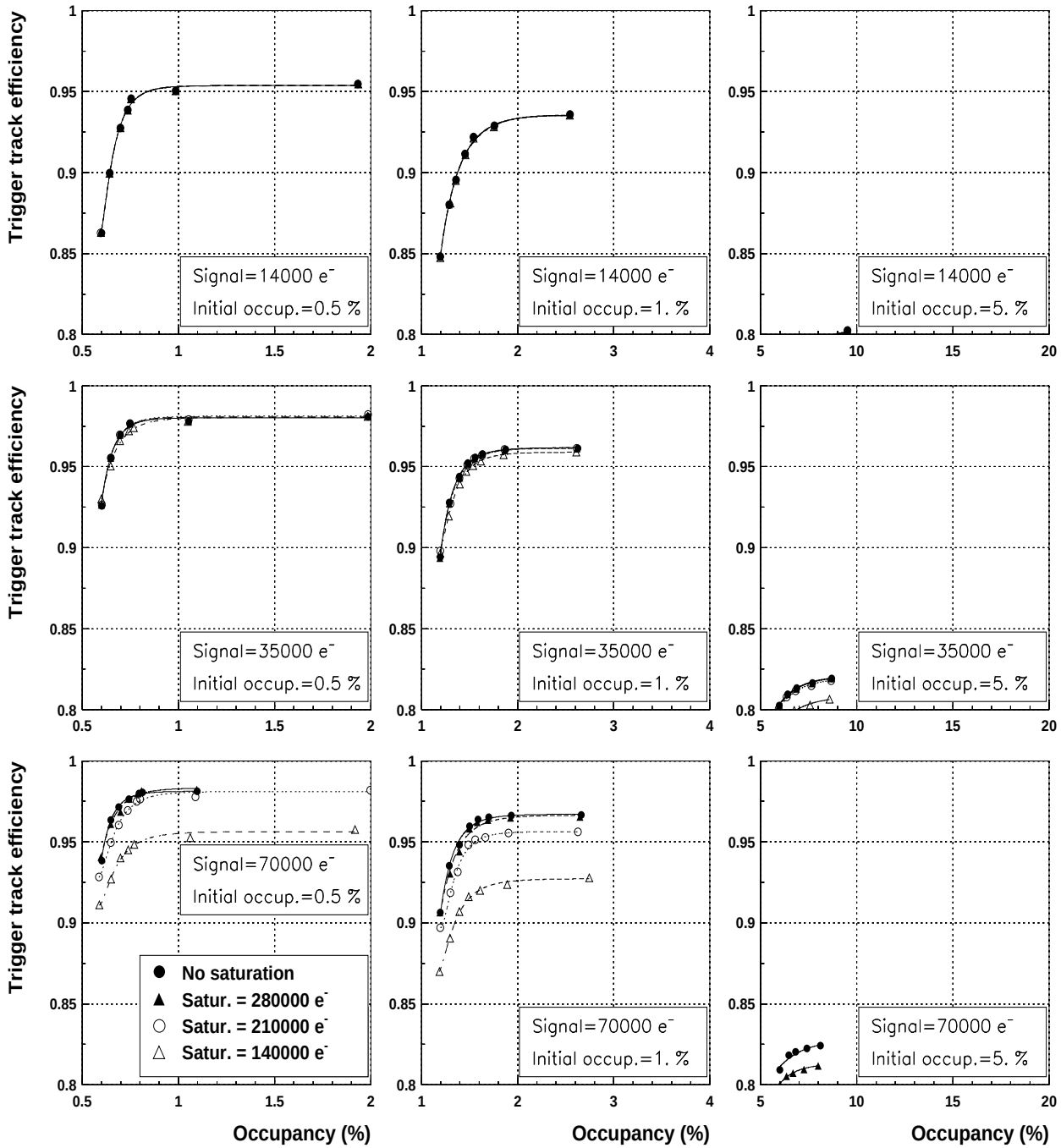

Figure 5b

Effect of the dynamical range on the performance of the shape identification algorithm in the case of the PRE-SHAP32 shaping. The noise rms is 1400 e^-.

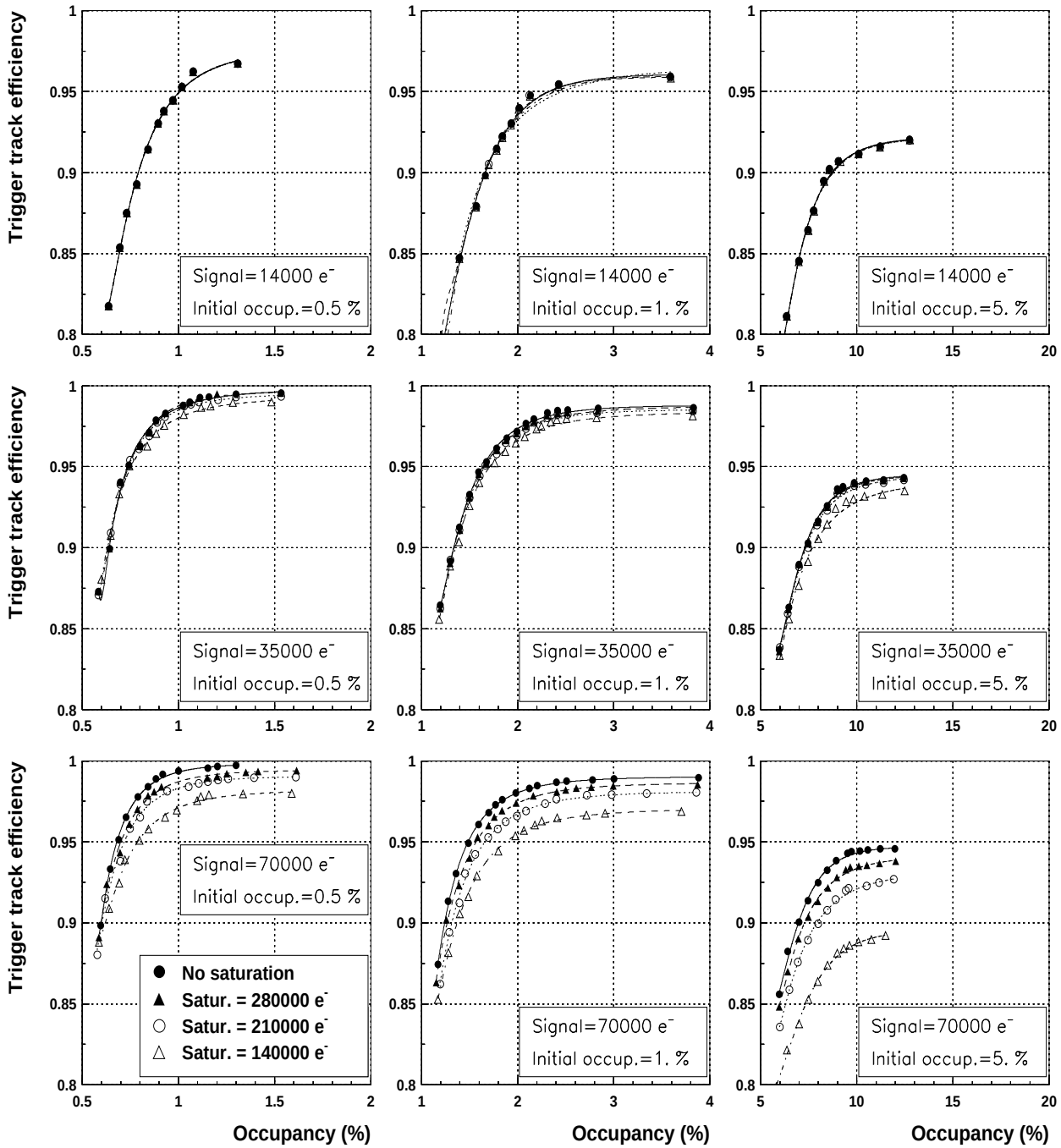

Figure 5c

Effect of the dynamical range on the performance of the rise selection algorithm in the case of the PRESHAPE32 shaping. The noise rms is 1400 e^-.

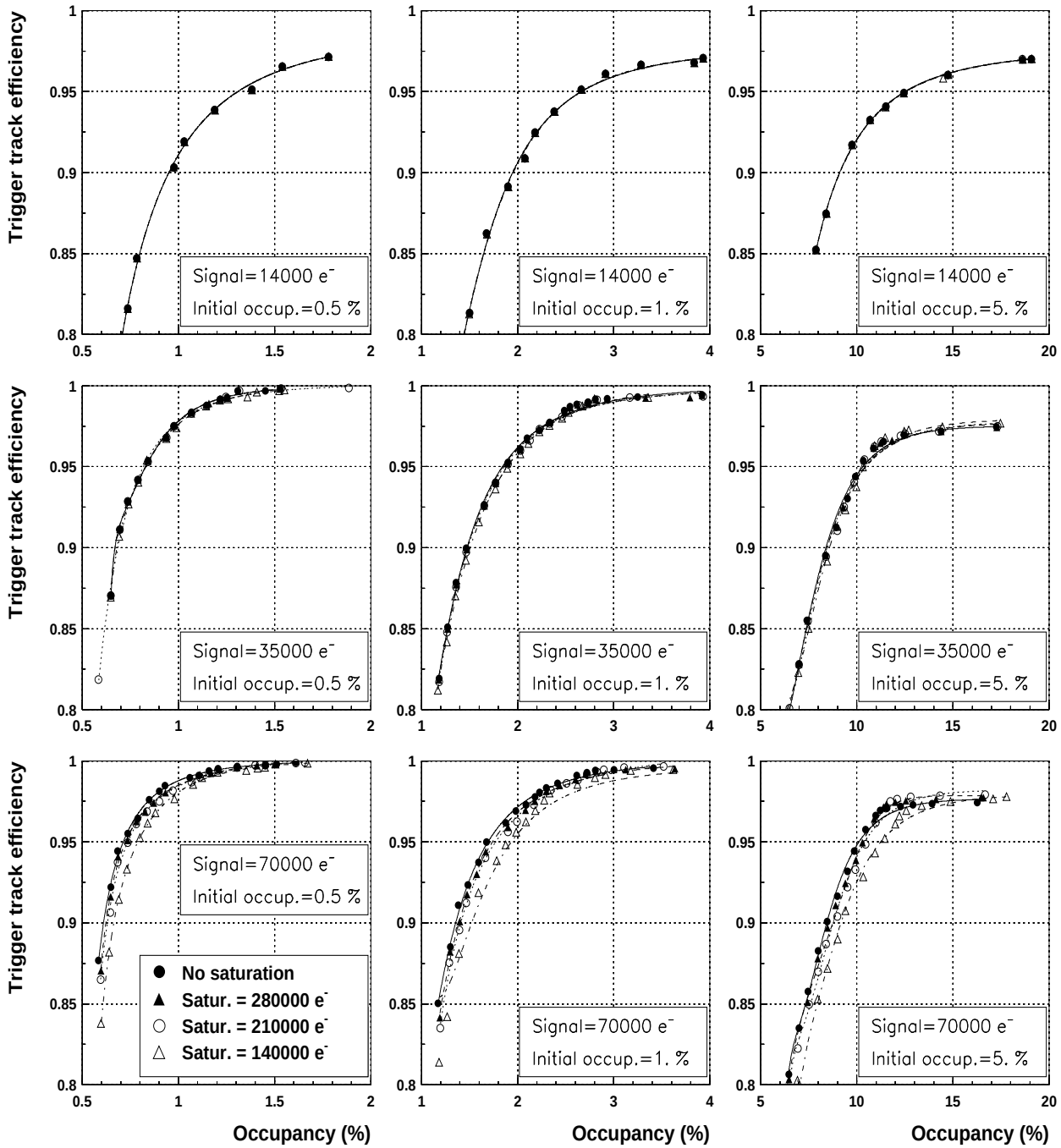

Figure 5d

Effect of the dynamical range on the performance of the weighted sum algorithm in the case of the PRESHAPE32 shaping. The noise rms is 1400 e^-.

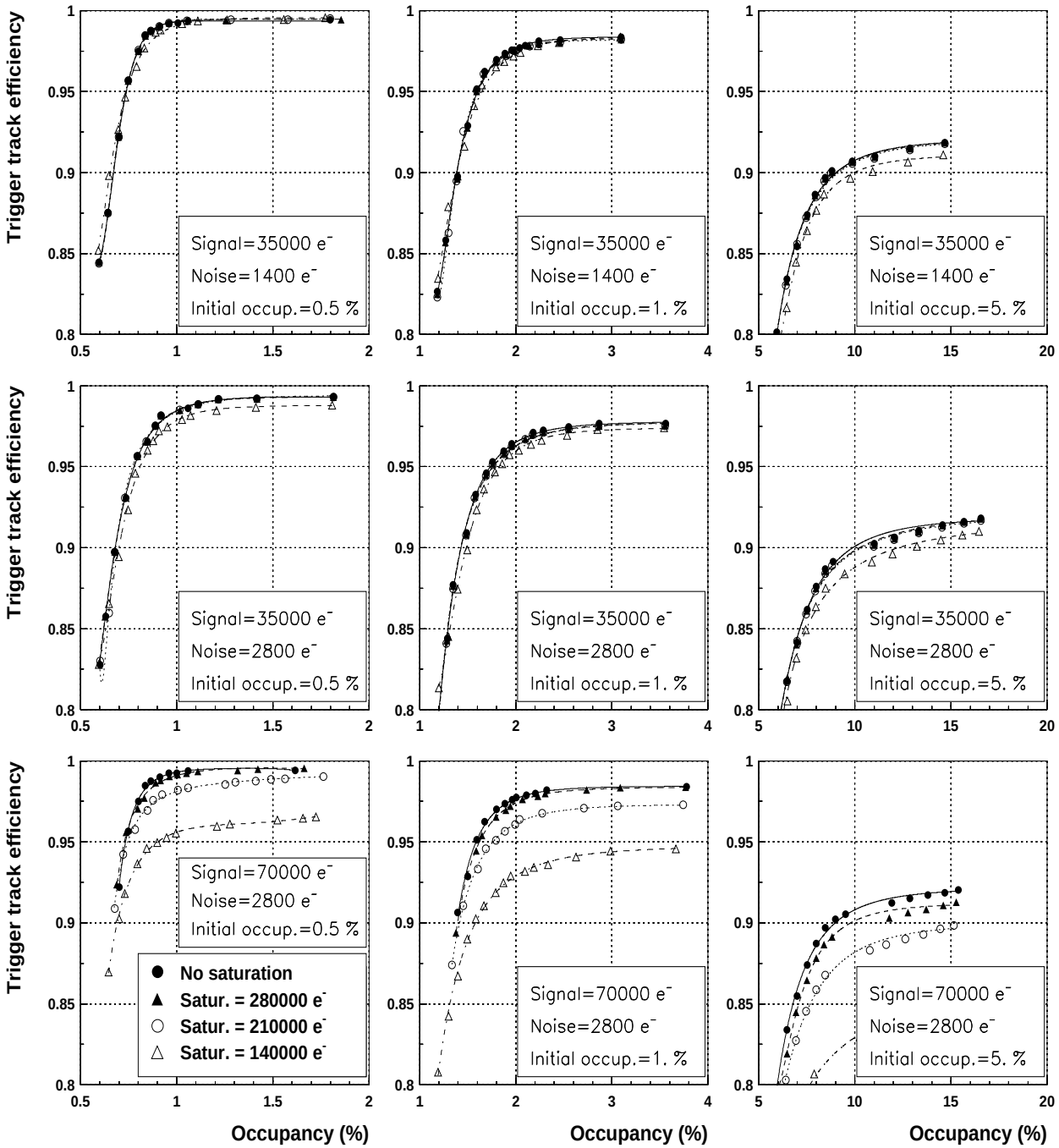

Figure 6a

Effect of the dynamical range on the performance of the peak identification algorithm in the case of the PRE-SHAPE32 shaping. Comparison for noise rms of 1400 e^- and 2800 e^-.

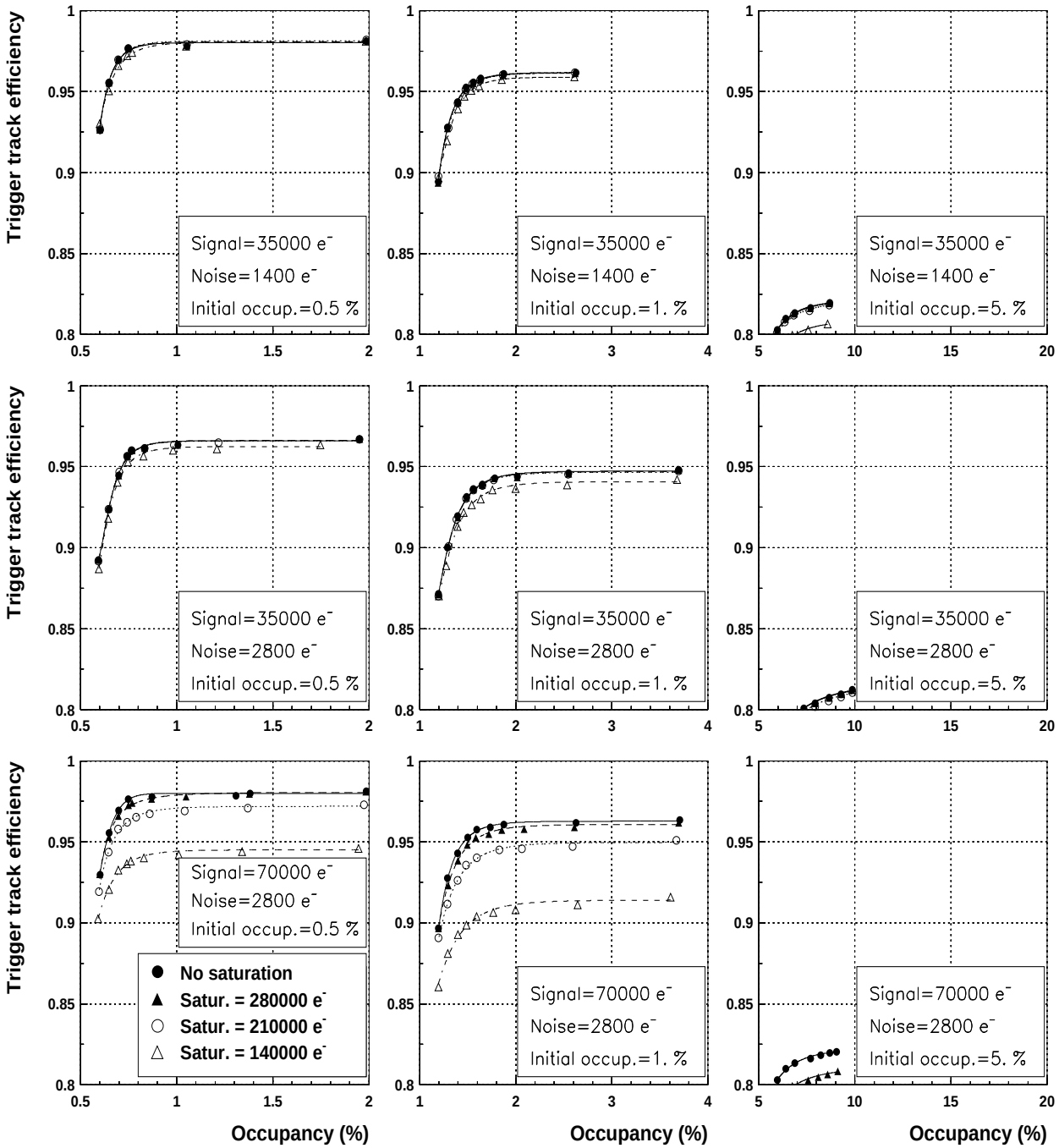

Figure 6b

Effect of the dynamical range on the performance of the shape identification algorithm in the case of the PRE-SHAPE32 shaping. Comparison for noise rms of 1400 e^- and 2800 e^-.

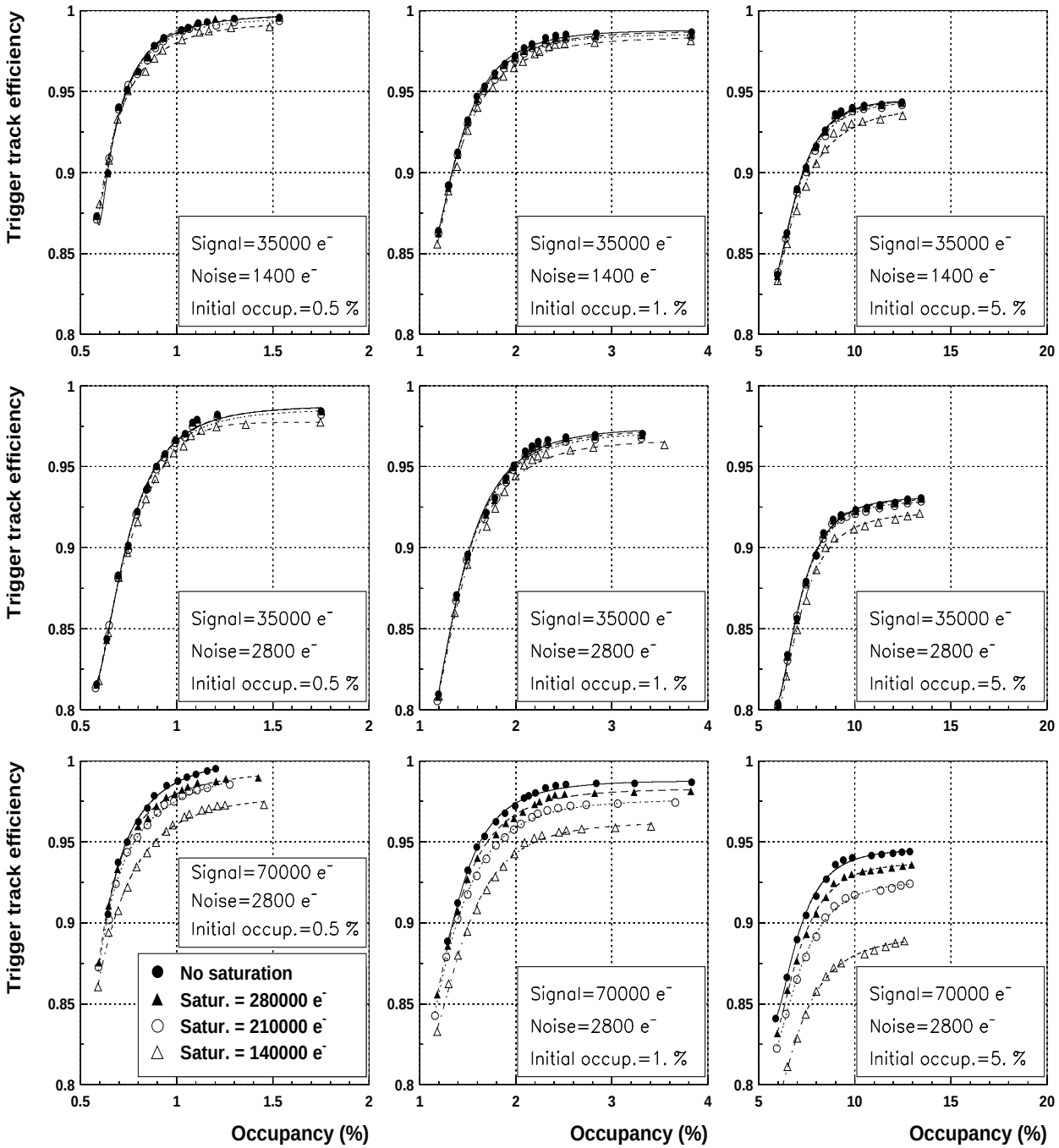

Figure 6c

Effect of the dynamical range on the performance of the rise selection algorithm in the case of the PRESHAPE32 shaping. Comparison for noise rms of 1400 e^- and 2800 e^-.

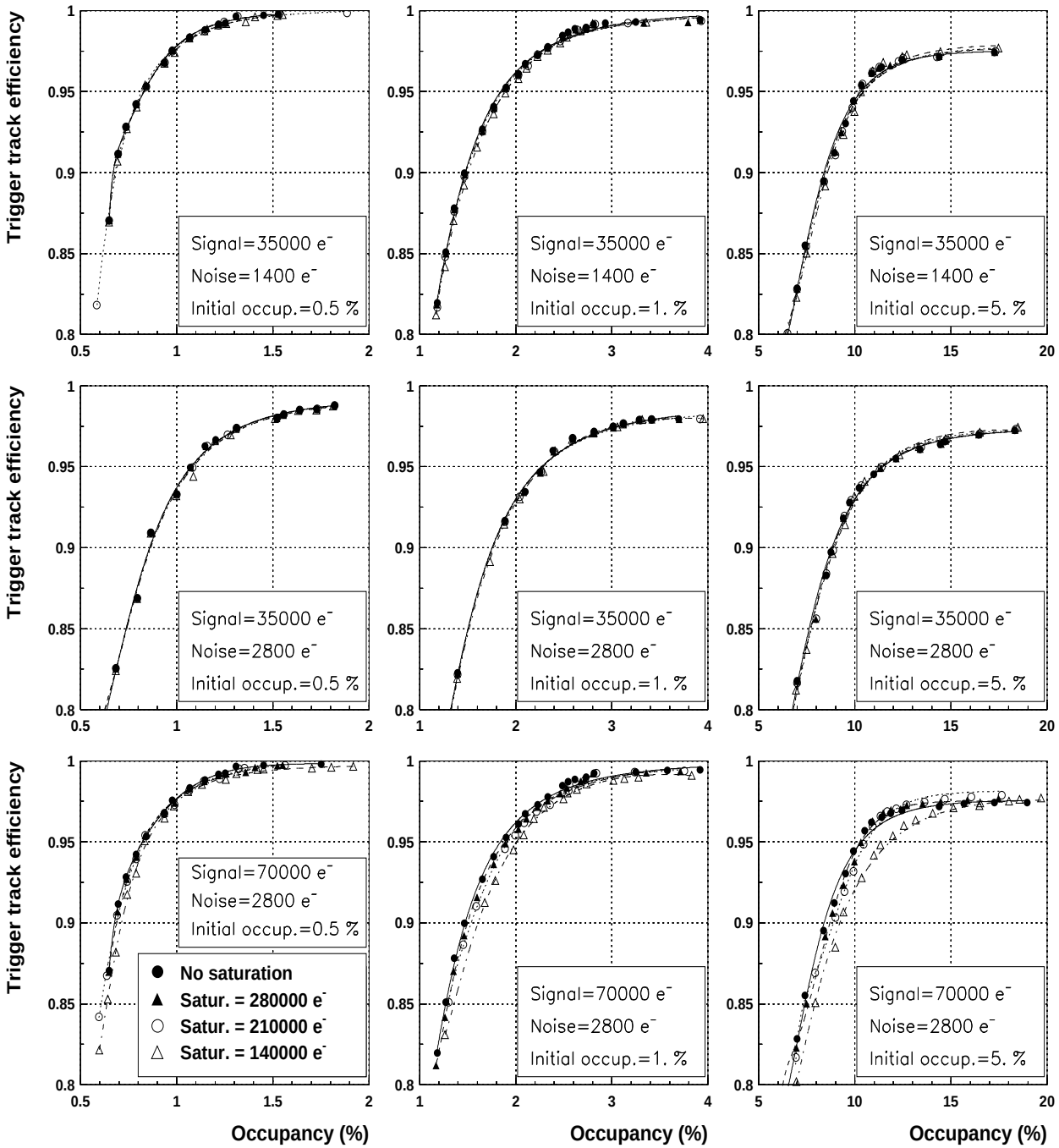

Figure 6d

Effect of the dynamical range on the performance of the weighted sum algorithm in the case of the PRESHAPE32 shaping. Comparison for noise rms of 1400 e^- and 2800 e^-.

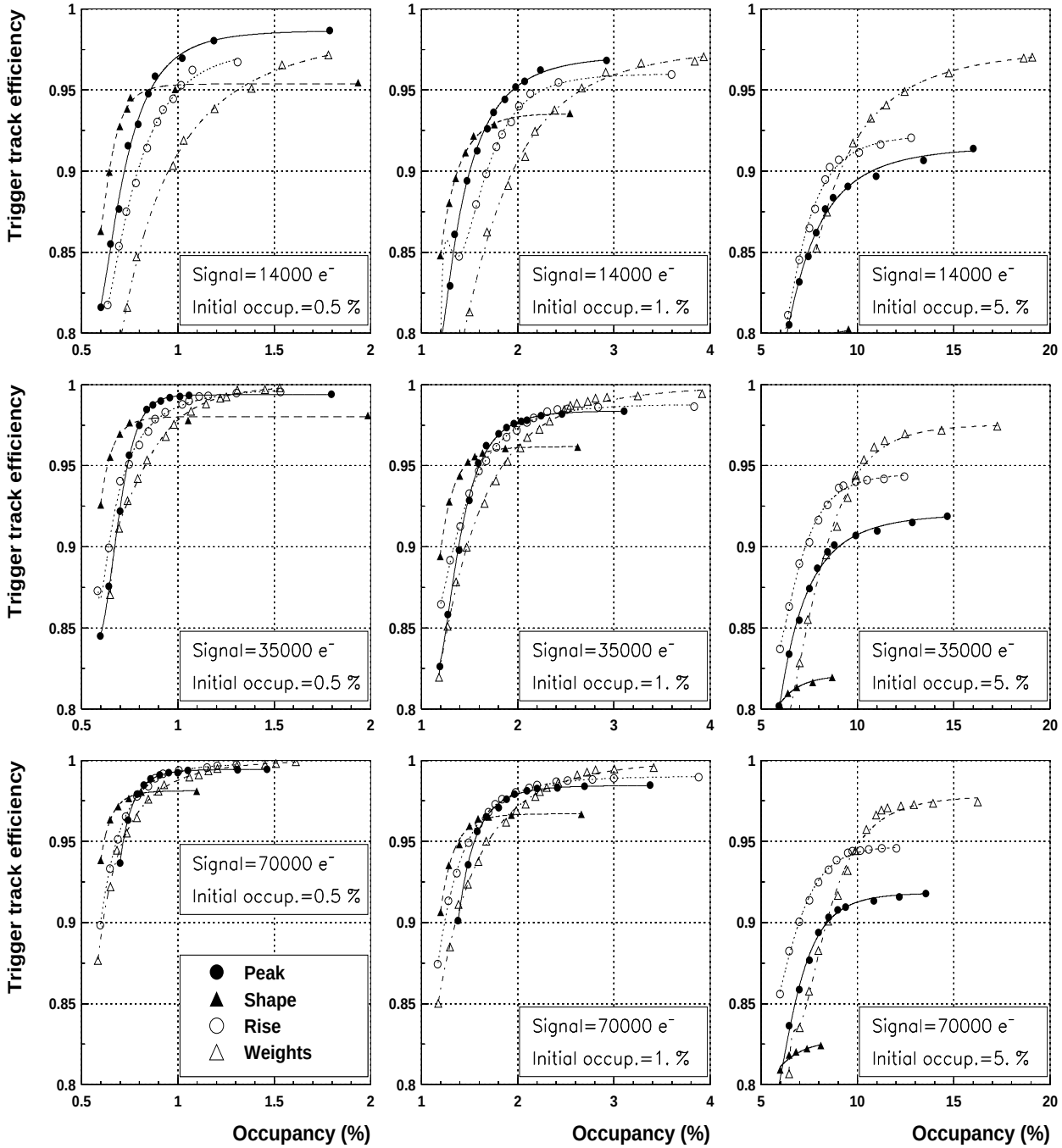

Figure 7

Comparison of the algorithms performance in the case of the PRESHAPE32 shaping. The noise rms is 1400 e^-.

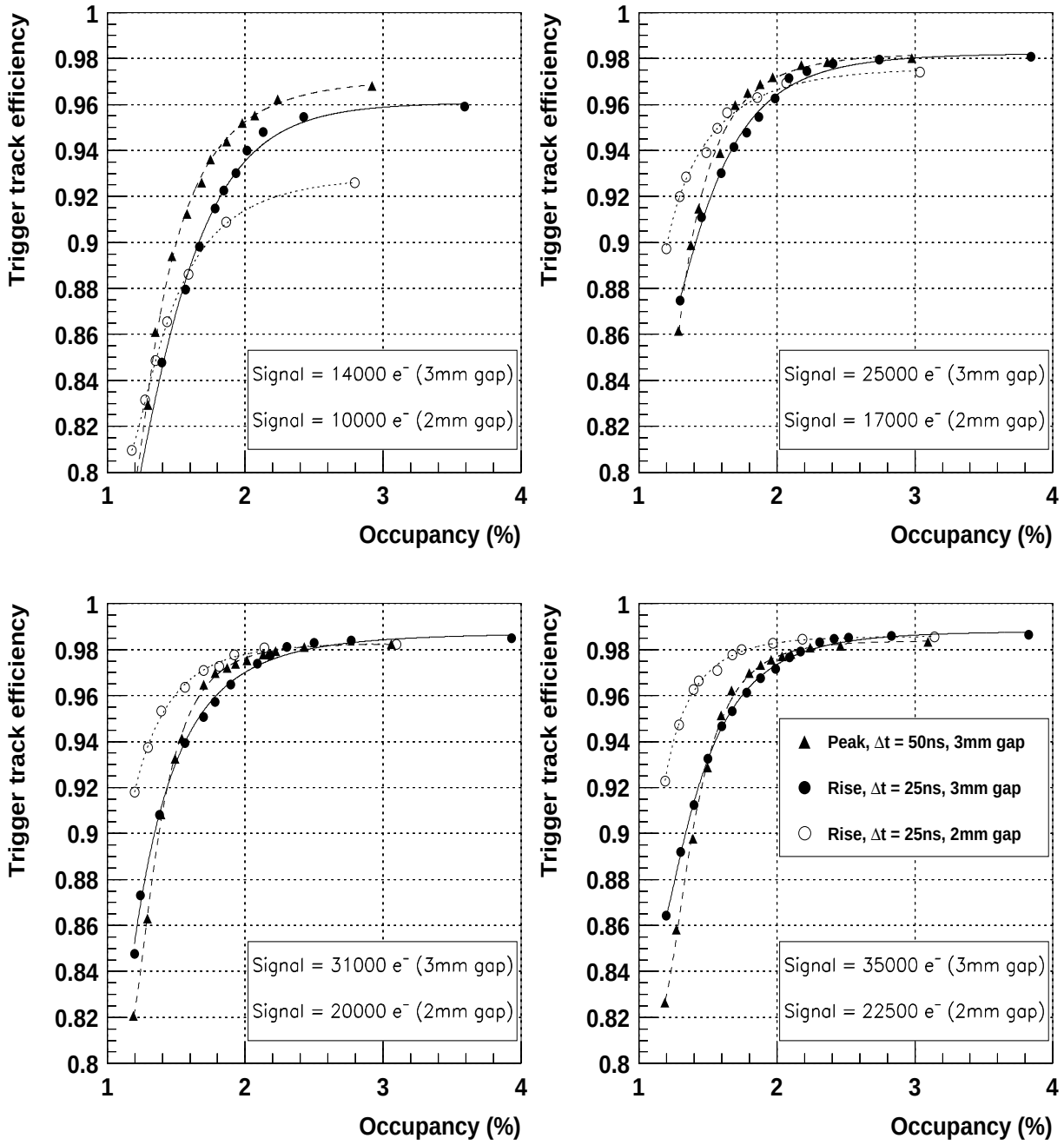

Figure 8

Comparison of the performance of the peak identification and the rise selection algorithms with 3 mm and 2 mm gas gaps and the PRESHAPE32 shaping. The noise rms is 1400 e^- and the initial detector occupancy is 1%.

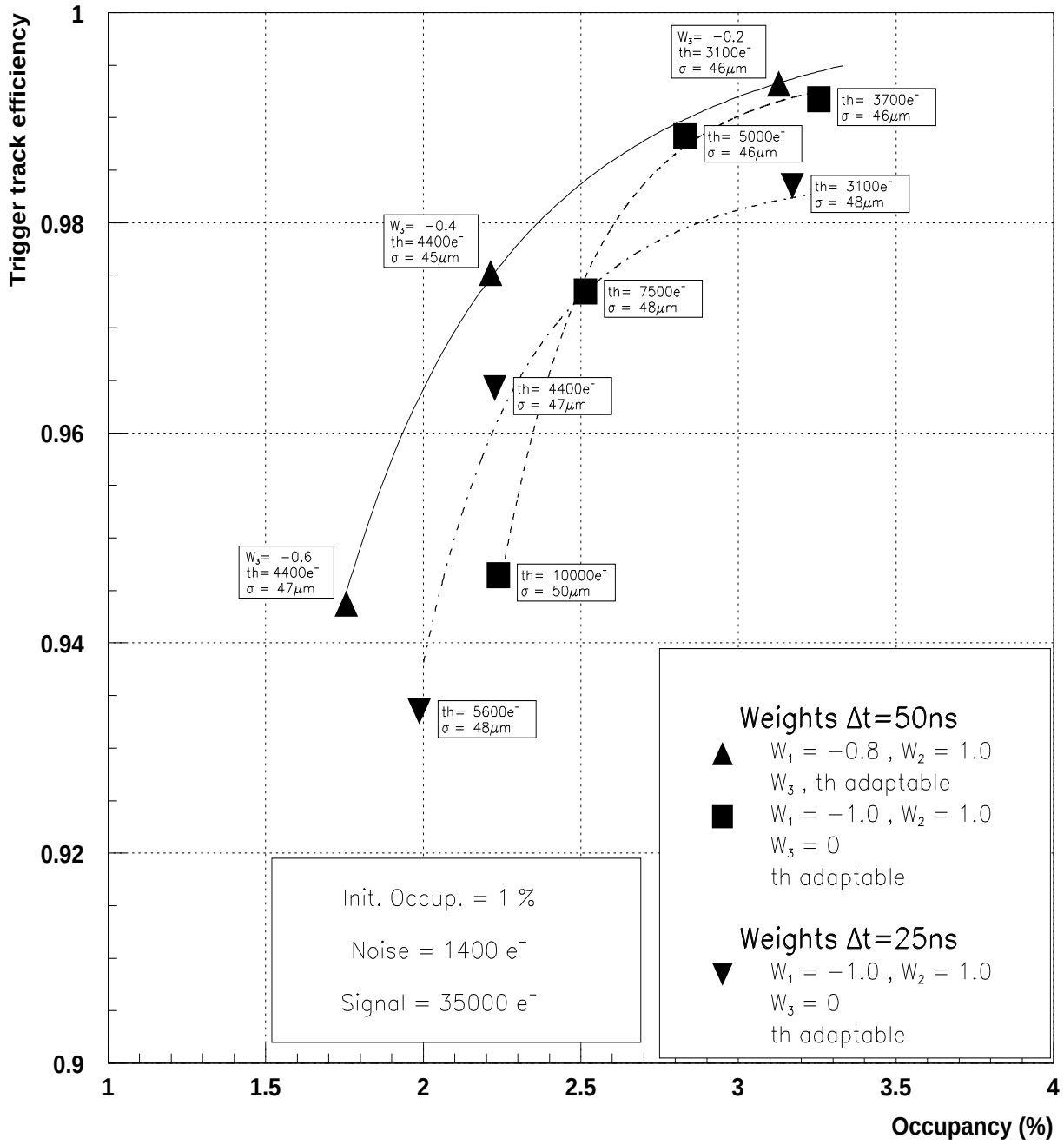

Figure 9

Performance and spatial resolution of the weighted sum obtained with the PRESHAPE32 shaping, using specific sets of weights and thresholds.

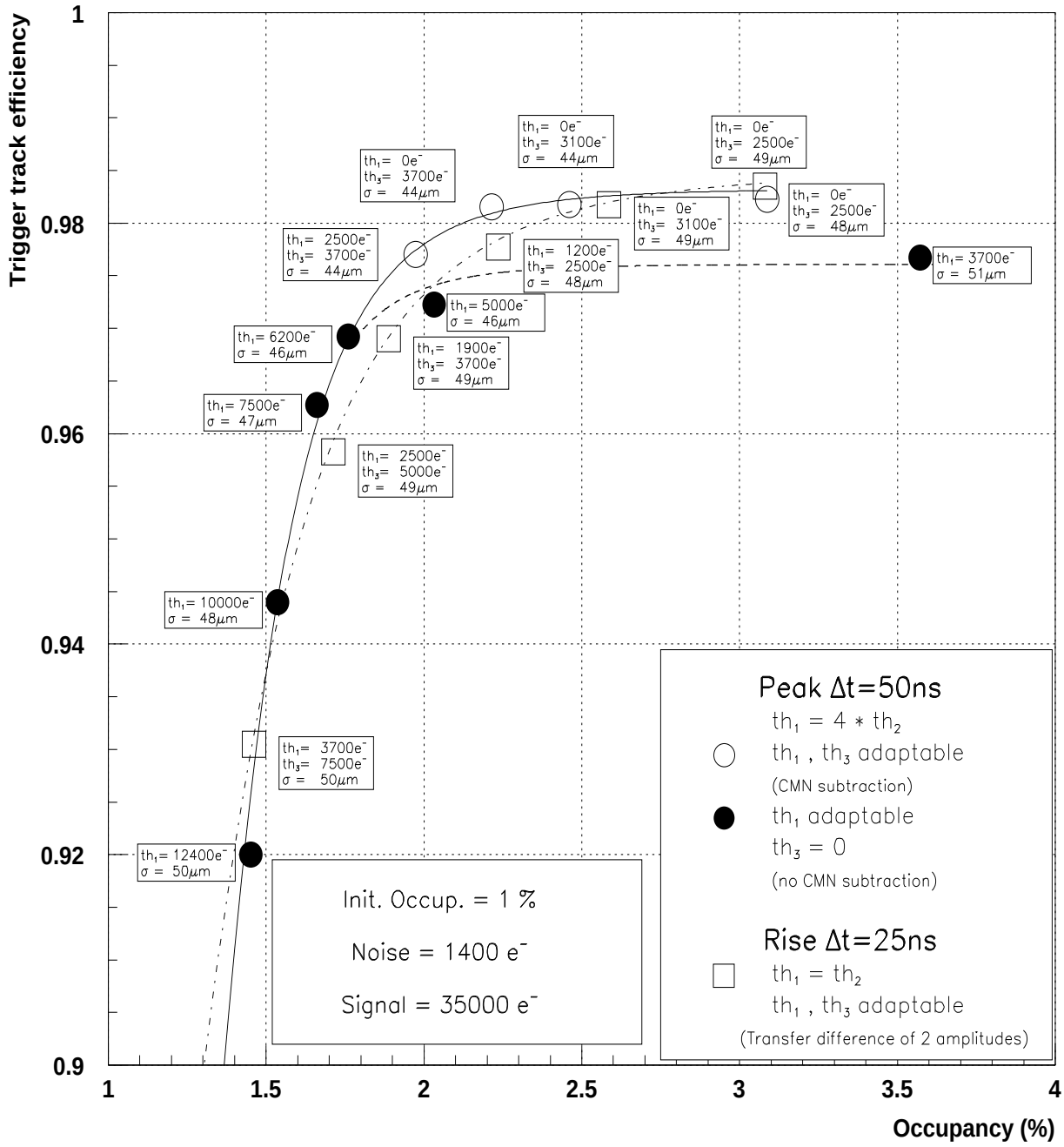

Figure 10

Performance and spatial resolution of the peak and rise selection obtained with the PRESHAPE32 shaping, using specific sets of thresholds to simulate the cases with and without common mode noise subtraction (see text).

Figure 11

Scheme of a possible implementation of the peak identification and the rise selection in a single chip.